

3-D Optical Measurement Using Phase Shifting Based Methods

Peisen S. Huang^a and Song Zhang^b

^a Department of Mechanical Engineering, SUNY at Stony Brook, Stony Brook, NY 11794-2300, Email: {peisen.huang}@stonybrook.edu

^b Department of Mathematics, Harvard University, Cambridge, MA 02138, Email: {szhang}@fas.harvard.edu

ABSTRACT

We review some of our most recent works on 3-D shape measurement using the digital fringe projection and phase-shifting method. First, we introduce the measurement principle and phase-shifting algorithms. Then we discuss an effective method for phase error compensation and a novel idea for system calibration. Finally, we describe a 3-D shape measurement system for high-resolution, real-time 3-D shape acquisition, reconstruction and display.

Keywords: 3-D shape measurement, phase-shifting method, phase error compensation, calibration, real-time 3-D shape measurement.

1. INTRODUCTION

3-D shape measurement techniques have numerous applications in many different areas, including reverse engineering, industrial inspection, entertainment, security, computer vision, etc. They can generally be classified into two groups: contact and non-contact methods. A typical contact method uses a coordinate measuring machine (CMM), which is widely used for dimensional inspection and quality control in manufacturing. CMMs are versatile metrology machines that can provide high measurement accuracy in large measurement volumes. However, these machines are usually slow and provide only limited data density. In addition, due to their contact nature, they cannot accurately measure flexible or soft objects such as thin sheet parts, rubber parts, biological objects, etc.¹ Compared to contact methods, non-contact methods do not have these limitations. Many non-contact 3-D shape measurement techniques have been developed, among which optical methods play an important role.²⁻⁴ Traditional optical methods include stereo vision,⁵ shape from shading,⁶ shape from focus and defocus,^{7,8} laser stripe scanning,⁹ structured light,¹⁰⁻¹² Moiré interferometries,¹³ and digital fringe projection and phase shifting.^{14,15} In recent years, with the widespread use of digital projectors, the digital fringe projection and phase-shifting method has attracted lots of interest due to its capability in providing high-resolution and high-speed 3-D shape measurement.

In this paper, we will review some of our recent works on 3-D shape measurement based on the digital fringe projection and phase-shifting method. We will discuss issues related to phase-shifting algorithms, phase error compensation, system calibration, and real-time 3-D shape measurement.

2. PRINCIPLE

Phase-shifting method has been used extensively in optical metrology to measure 3-D shapes of objects at various scales. In this method, a series of phase-shifted sinusoidal fringe patterns are recorded, from which the phase information at every pixel is obtained. This phase information is then converted to xyz coordinates of the object surface after the system is calibrated.

Traditionally, fringe patterns are produced mostly by use of light interference or gratings. In recent years, with the increasingly ubiquitous availability of projectors, more and more researchers start to use projectors to generate fringe patterns. Figure 1 shows a typical system setup. A projector projects a series of computer-generated, phase-shifted fringe patterns onto the object. The fringe patterns deformed by the object surface are

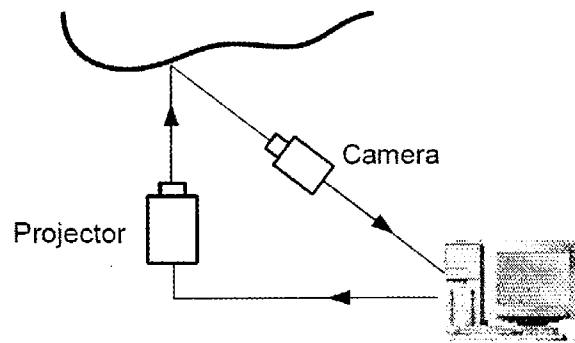


Figure 1. 3-D shape measurement system based on the digital fringe projection and phase-shifting method.

captured by a camera. Then a phase-wrapping and -unwrapping algorithm and a phase-to-coordinates conversion algorithm are used to reconstruct the 3-D geometry. Figure 2 shows example results of measuring a sculpture of Lincoln using this method. The phase-shifting algorithm used is the three-step algorithm (will be discussed later) with a phase shift of 120° . Major advantages of using a projector in such a system include the easiness and flexibility in generating fringe patterns as well as the digital accuracy of phase shifting.

3. PHASE-SHIFTING ALGORITHMS

Many different phase-shifting algorithms have been developed in the past.¹⁶ The general form of these algorithms is the least square algorithm. Let us assume that a total of N phase-shifted fringe images are captured, each with a phase shift of δ_i ($i = 1, 2, \dots, N$). Then the intensity of the i -th image can be represented as

$$I_i(x, y) = I'(x, y) + I''(x, y) \cos[\phi(x, y) + \delta_i], \quad (1)$$

where $I'(x, y)$ is the average intensity, $I''(x, y)$ the intensity modulation, and $\phi(x, y)$ the phase to be determined. By solving Eq. (1) simultaneously by the least square algorithm, we can obtain the phase

$$\phi(x, y) = \tan^{-1} \left(\frac{-a_2(x, y)}{a_1(x, y)} \right), \quad (2)$$

and the data modulation

$$\gamma(x, y) = \frac{I''(x, y)}{I'(x, y)} = \frac{[a_1(x, y)^2 + a_2(x, y)^2]^{1/2}}{a_0(x, y)}, \quad (3)$$

where

$$\begin{bmatrix} a_0(x, y) \\ a_1(x, y) \\ a_2(x, y) \end{bmatrix} = \mathbf{A}^{-1}(\delta_i) \mathbf{B}(x, y, \delta_i), \quad (4)$$

$$\mathbf{A}(\delta_i) = \begin{bmatrix} N & \sum \cos(\delta_i) & \sum \sin(\delta_i) \\ \sum \cos(\delta_i) & \sum \cos^2(\delta_i) & \sum \cos(\delta_i) \sin(\delta_i) \\ \sum \sin(\delta_i) & \sum \cos(\delta_i) \sin(\delta_i) & \sum \sin^2(\delta_i) \end{bmatrix}, \quad (5)$$

and

$$\mathbf{B}(x, y, \delta_i) = \begin{bmatrix} \sum I_i \\ \sum I_i \cos(\delta_i) \\ \sum I_i \sin(\delta_i) \end{bmatrix}. \quad (6)$$

Other phase-shifting algorithms, such as the three-step, four-step, Carré, 3+3, Hariharan, 2+1, double three-step,¹⁶ etc., can be regarded as the special cases of the least-square algorithm when N and δ_i take different values. For the digital fringe projection method, which uses a projector to generate the phase-shifted fringe

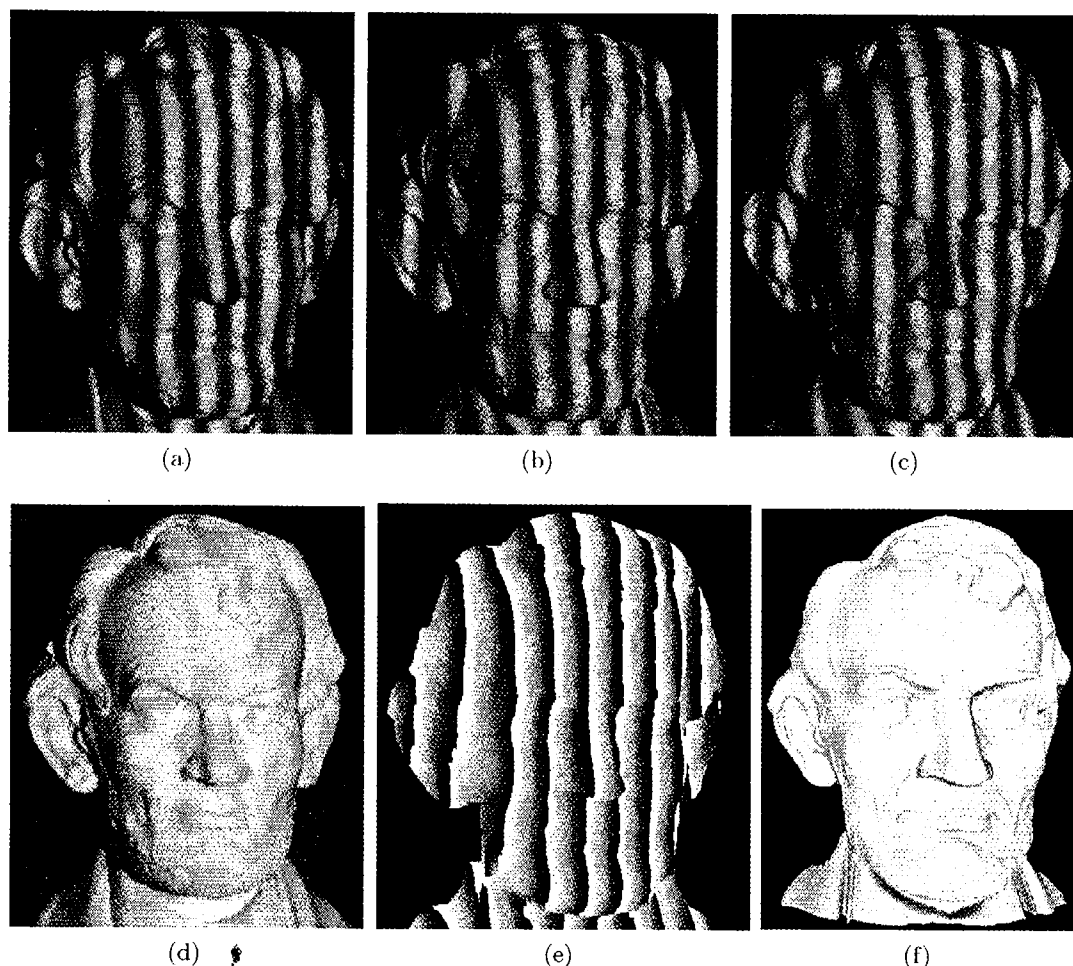


Figure 2. Measurement results of a Lincoln head sculpture. (a) Fringe image $I_1(\alpha = -120^\circ)$. (b) Fringe image $I_2(\alpha = 0^\circ)$. (c) Fringe image $I_3(\alpha = 120^\circ)$. (d) 2-D photo. (e) Wrapped phase map. (f) 3-D shape after phase-unwrapping.

patterns, we found that the three-step algorithm with $\delta_i = -2\pi/3, 0, 2\pi/3$ produced the best result.¹⁷ In this case, Eqs.(2) and (3) for calculating the phase and data modulation become

$$\phi(x, y) = \tan^{-1} \left(\sqrt{3} \frac{I_1 - I_3}{2I_2 - I_1 - I_3} \right), \quad (7)$$

and

$$\gamma(x, y) = \frac{I''(x, y)}{I'(x, y)} = \frac{[3(I_1 - I_3)^2 + (2I_2 - I_1 - I_3)^2]^{1/2}}{I_1 + I_2 + I_3}, \quad (8)$$

Phase $\phi(x, y)$ in Eqs. (2) and (7) is the so-called modulo 2π phase at each pixel whose value ranges from 0 to 2π . If the fringe patterns contain multiple fringes, phase unwrapping is necessary to remove the sawtooth-like discontinuities and obtain a continuous phase map.¹⁸ Once the continuous phase map is obtained, the phase at each pixel can be converted to xyz coordinates of the corresponding point on the object surface through calibration.¹⁹⁻²¹ The average intensity $I'(x, y)$ represents a flat image of the measured object and can be used for texture mapping in computer vision and computer graphics applications. Data modulation $\gamma(x, y)$ has a value between 0 and 1 and can be used to determine the quality of the phase data at each pixel with 1 being the best.

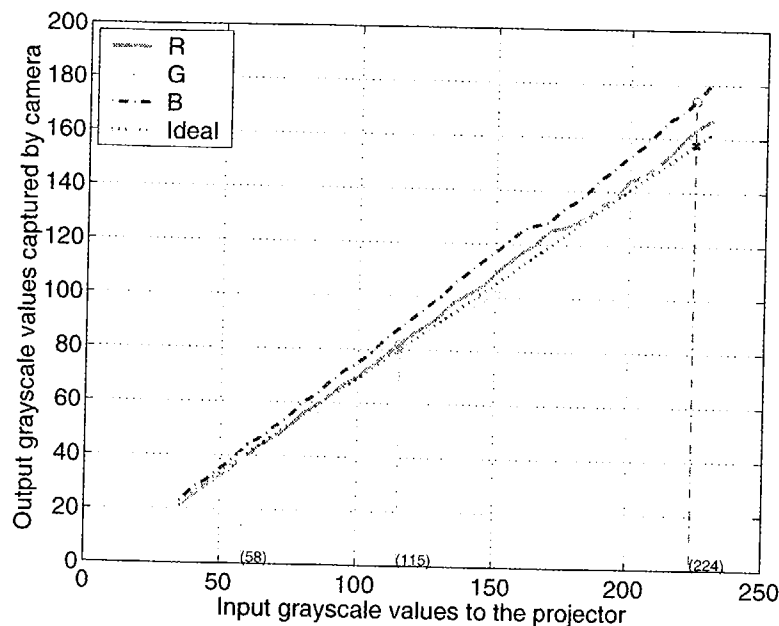


Figure 3. Measured gamma curves of the projector.

4. PHASE ERROR COMPENSATION

The measurement accuracy of a phase-shifting method is usually affected by such error sources as the phase shift error,²²⁻²⁴ non-sinusoidal waveforms,²⁵ camera noise and nonlinearity,²⁶ vibration,²⁷ speckle noise,²⁸ etc. In the digital fringe projection and phase-shifting method, non-sinusoidal waveform is the single dominant error source. It results from the nonlinearity of the gamma curve of the projector and can cause significant phase measurement error. Previously proposed methods, such as the double three-step phase-shifting algorithm¹⁷ and the direct correction of the nonlinearity of the projector's gamma curve,¹⁴ were successful in significantly reducing the phase measurement error, but the residual error remains non-negligible. Zhang and Huang recently proposed a generic method that could in theory completely remove the phase error caused by nonlinear gamma curve of the projector.²⁹ This phase error compensation method is based on the finding that the phase error due to the non-sinusoidal waveform of the fringe patterns depends only on the nonlinearity of the projector's gamma curve. Therefore, if the projector's gamma curve is calibrated and the phase error due to the nonlinearity of the gamma curve is calculated, a look-up-table (LUT) that stores the phase error can be constructed for error compensation. Experimental results demonstrated that by using this method, the measurement error could be reduced by 10 times. Figure 3 shows a typical example of the measured gamma curves for the R, G, and B channels of the projector, which are visibly nonlinear. Figure 4 shows example results of measurement before and after phase error correction. It can be seen that the measurement error after phase error compensation is significantly reduced.

5. SYSTEM CALIBRATION

The key to accurate 3-D shape measurement using a camera and a projector is the proper calibration of the parameters as well as geometric relationship of the camera and projector.¹⁹ Figure 5 shows the model of a typical 3-D shape measurement system based on the digital fringe projection method. A camera or a projector is often described by a pinhole model using the intrinsic and extrinsic parameters. The intrinsic parameters include the focal length (f^c or f^p), the principle point ((u_0^c, v_0^c) or (u_0^p, v_0^p)), the pixel skew factor, and the pixel size. The extrinsic parameters include the rotation and translation matrices between the world coordinate system ($o^w; x^w y^w z^w$) and the camera coordinate system ($o^c; x^c y^c z^c$) or the projector coordinate system ($o^p; x^p y^p z^p$). Methods based on neural networks,^{30,31} bundle adjustment,³²⁻³⁷ or absolute phase²⁰ have been developed. In

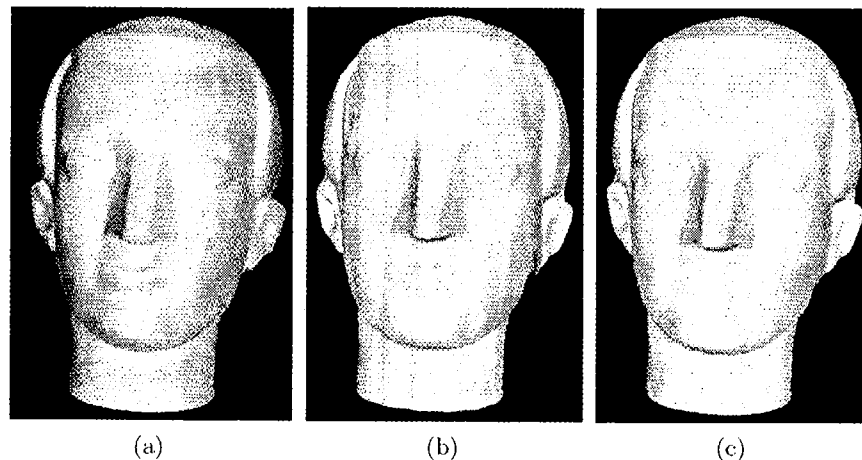


Figure 4. Reconstructed 3-D geometries of the head model before and after phase error compensation. (a) 2-D photo. (b) 3-D geometry before phase error compensation. (c) 3-D geometry after phase error compensation.

these methods, the calibration process varies depending on the available system parameters information and the system setup and involves complicated and time-consuming procedures.

Recently, Zhang proposed a novel and more systematic method for accurate and quick calibration of such systems.²¹ The core idea is to enable a projector to "capture" images like a camera, thus making the calibration of a projector the same as that of a camera, which is well established. To enable the projector to "capture" images, a camera is used to take the image for the projector. The image is then mapped to the projector to create the so-called projector image. The mapping relationship between the camera and the projector is established by using the phase-shifting method. This new method allows the projector and the camera to be calibrated independently, thus avoiding the problems related to the coupling of the camera and projector errors. By treating the projector as a camera, this method essentially unified the calibration procedures of any structure light system that uses a projector and a classic stereo vision system. In the experiment, a linear model with a small error look-up-table (LUT) was found to be sufficient to produce a reasonably accurate calibration result with an error of RMS 0.22 mm over a volume of $342(\text{H}) \times 376(\text{V}) \times 658(\text{D})$ mm. Figure 6 shows an example of the measurement result using this calibration method.

6. REAL-TIME 3-D SHAPE MEASUREMENT

A real-time 3-D shape measurement system can be used to capture 3-D shapes of dynamically changing objects, such as human faces and bodies. It can also be used to increase measurement throughput and avoid vibration-induced measurement errors in industrial inspection applications. In the digital fringe projection and phase-shifting method, real-time 3-D shape measurement can be realized by rapidly capturing the fringe images required to reconstruct the 3-D shape. As the phase-shifting algorithm, the three-step algorithm is normally the choice because it requires the minimum number of fringe images. To rapidly capture the fringe images, one method is to use color. The three phase-shifted fringe patterns can be encoded in the three primary color channels of a projector.³⁸ By using a color camera to capture the color fringe pattern and then separating it into three color channels, one can acquire the fringe patterns simultaneously. However, the measurement accuracy is usually affected by the surface color of the object. Another method is to switch B/W fringe patterns rapidly so that three fringe images can be captured in real time. Huang *et al.* proposed a method using a single-chip DLP projector to project three phase-shifted fringe patterns and a B/W CCD camera synchronized with the projector to capture the fringe images rapidly.¹⁴ The achieved speed was 16 frames per second. Recently, Zhang and Huang significantly improved the system and realized a 3-D data acquisition speed at 40 frames per second with an image resolution of 532×500 .¹⁵ This speed is fast enough for measuring objects with slowly changing surface geometry, such as human facial expressions. Figure 7 shows 8 frames of the reconstructed 3-D models of a human

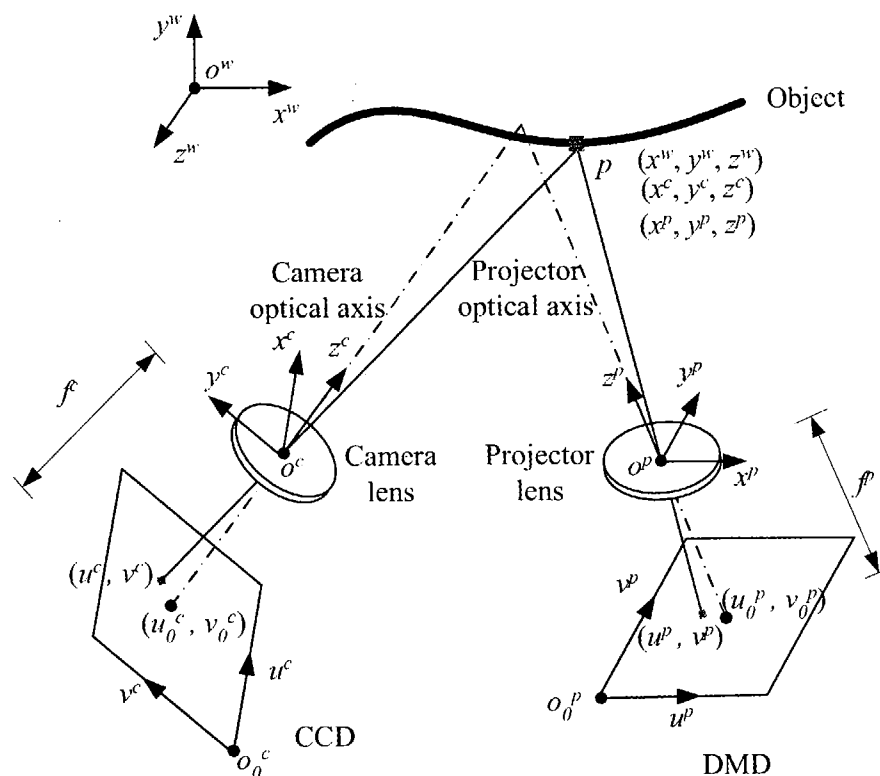


Figure 5. Model of the 3-D shape measurement system.

face. During the acquisition, the subject was asked to smile so that facial changes were introduced. It can be seen that detailed facial expression changes have been successfully captured.

To realize a true real-time 3-D shape measurement system, in which not only the fringe images are acquired in real time, but also the 3-D shape reconstruction and display are done in real time, we developed new three-step phase-shifting algorithms to improve the processing speed. The traditional three-step algorithm that calculates the phase using an arctangent function was found to be too slow for real-time processing. To solve this problem, Huang *et al.* proposed an intensity ratio based phase-shifting method, namely, trapezoidal phase-shifting method, for faster processing speed.³⁹ Figure 8 shows a measurement result using this method. The 3-D reconstruction speed was reported to be 4.5 times faster. However, the measurement accuracy is affected by image defocusing, although the error is small. To retain the speed advantage of the trapezoidal phase-shifting method while improving the measurement accuracy, Huang and Zhang recently proposed to use the trapezoidal phase-shifting algorithm to process the sinusoidal fringe patterns and then use a look-up-table (LUT) to compensate for the resulting phase error.⁴⁰ Experimental results showed that this new algorithm provided similar measurement accuracy as the traditional algorithm, but was 3.4 times faster.

The adoption of this new algorithm enabled us to successfully build a high-resolution, real-time 3-D shape measurement system that captures, reconstructs, and displays the 3-D shape of an object at a speed of 40 fps and a resolution of 532×500 pixels, all with an ordinary personal computer.²¹ Figure 9(a) shows the experimental environment of the real-time 3-D system. A projector was utilized to project the computer screen onto a white board on the side of the object. Figure 9(b) shows one image of a video sequence recorded during the experiments. The image on the left is the face of a human subject, while the image on the right is the image generated by the system in real time.

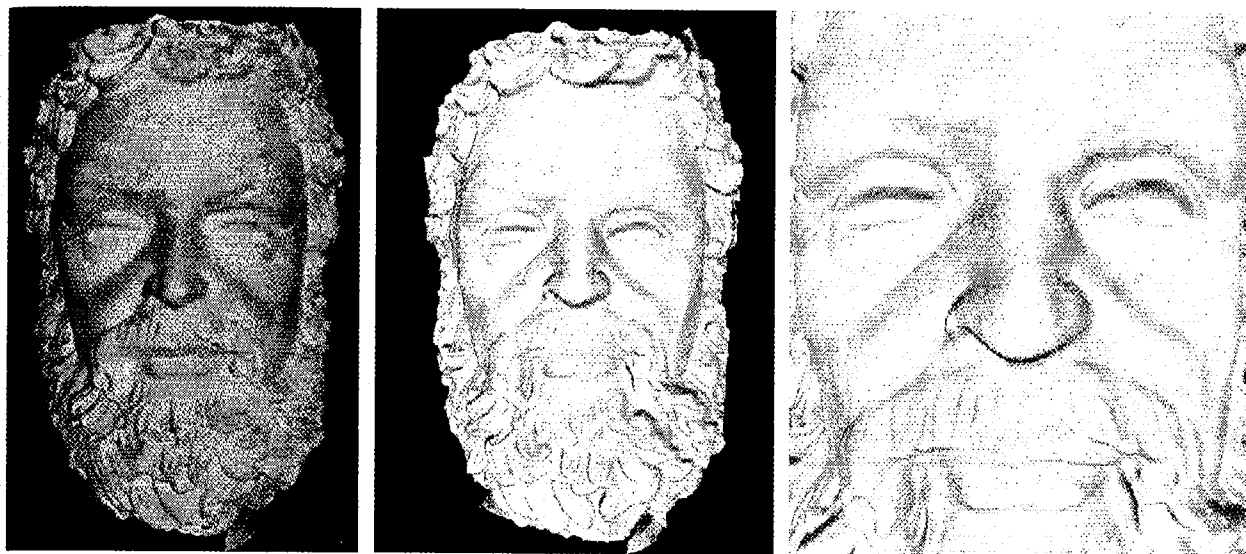


Figure 6. 3-D measurement result of the sculpture Zeus. (a) 2-D photo. (b) 3-D geometry. (c) Zoom in view of the 3-D geometry .

7. CONCLUSIONS

In this paper, we reviewed some of our recent developments on the 3-D shape measurement technique based on a digital fringe projection and phase-shifting method. We focused our discussions on the techniques we proposed to improve measurement accuracy and speed. In particular, we described an effective method for phase error compensation, a novel idea for system calibration, and also the capabilities and applications of a high-resolution, real-time system for 3-D shape measurement we developed recently. Digital fringe projection and phase-shifting method has many advantages when compared to other traditional methods for 3-D shape measurement. We believe that it will find many real applications in various fields.

ACKNOWLEDGMENTS

This work was supported by the National Science Foundation under grant No. CMS-9900337 and National Institute of Health under grant No. RR13995.

REFERENCES

1. Q. Hu, *3-D Shape Measurement Based on Digital Fringe Projection and Phase-Shifting Techniques*. PhD thesis, State University of New York at Stony Brook, Stony Brook, NY, 11794, 2001.
2. F. Chen, G. M. Brown, and M. Song, "Overview of three-dimensional shape measurement using optical method," *Opt. Eng.* **39**(1), pp. 10-22, 2000.
3. K. G. Harding, "Color encoded morié contouring," in *Proc. SPIE*, **1005**, pp. 169-178, 1988.
4. Y. Y. Hung, L. Lin, H. M. Shang, and B. G. Park, "Practical three-dimensional computer vision techniques for full-field surface measurement," *Opt. Eng.* **39**(1), pp. 143-149, 2000.
5. U. Dhond and J. Aggarwal, "Structure from stereo-a review," *IEEE Trans. Systems, Man, and Cybernetics* **19**(6), pp. 1489-1510, 1989.
6. R. Zhang, P.-S. Tsai, J. Cryer, and M. Shah, "Shape from shading: A survey," *IEEE Trans. on Pattern Analysis and Machine Intelligence* **21**, pp. 690-706, Aug. 1999.
7. M. Subbarao and T. Choi, "Focusing techniques," in *Proc. of SPIE*, pp. 163-174, 1992.
8. M. Subbarao and G. Surya, "Application of spatial-domain convolution/deconvolution transform for determining distance from image defocus," in *Proc. of SPIE*, pp. 159-167, 1992.



Figure 7. Measurement results of facial expressions.

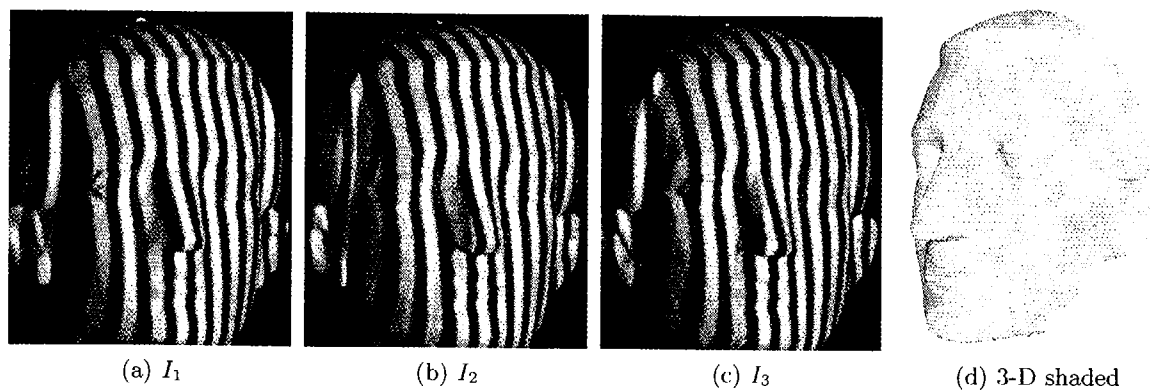


Figure 8. 3-D shape measurement of a plaster sculpture using the trapezoidal phase-shifting method.

9. M. Levoy, K. Pulli, B. Curless, S. Rusinkiewicz, D. Koller, L. Pereira, M. Ginzton, S. Anderson, J. Davis, J. Ginsberg, J. Shade, and D. Fulk, "The digital michelangelo project," in *Proceedings of SIGGRAPH 2000*, K. Akeley, ed., *Computer Graphics Proceedings, Annual Conference Series*, pp. 131-144, ACM, ACM Press / ACM SIGGRAPH, 2000.
10. J. Batlle, E. M. Mouaddib, and J. Salvi, "Recent progress in coded structured light as a technique to solve the correspondence problem: A survey," *Pattern Recognition*, pp. 1-63, 1998.

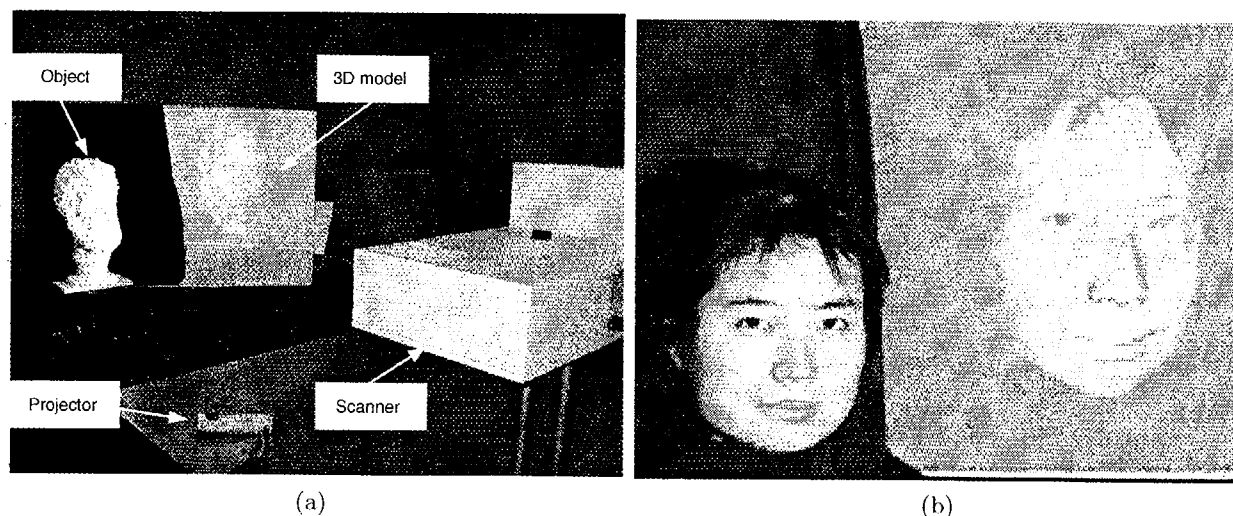


Figure 9. Real-time 3-D shape acquisition, reconstruction, and display. (a) Experimental setup. (b) Experiment on real-time facial expression capture.

11. B. Curless, "Overview of active vision techniques," in *Proc. SIGGRAPH 99 Course on 3D Photography*, 1999.
12. J. Davis, R. Ramamoorthi, and S. Rusinkiewicz, "Spacetime stereo: A unifying framework for depth from triangulation," *IEEE Trans. on Pattern Analysis and Machine Intelligence* **27**(2), pp. 1-7, 2005.
13. L. H. Bieman, "Survey of design consideration for 3d imaging system," in *Proc. SPIE, Optics, illumination, and image sensing for machine vision III* **1005**, pp. 138-144, 1988.
14. P. S. Huang, C. Zhang, and F. P. Chiang, "High-speed 3-d shape measurement based on digital fringe projection," *Opt. Eng.* **42**(1), pp. 163-168, 2003.
15. S. Zhang and P. Huang, "High-resolution, real-time dynamic 3-d shape acquisition," in *IEEE Computer Vision and Pattern Recognition Workshop (CVPRW'04)*, **3**(3), pp. 28-37, 2004.
16. D. Malacara, ed., *Optical Shop Testing*, John Wiley and Sons, NY, 1992.
17. P. S. Huang, Q. Y. Hu, and F. P. Chiang, "Double three-step phase-shifting algorithm," *Appl. Opt.* **41**(22), pp. 4503-4509, 2002.
18. D. C. Ghiglia and M. D. Pritt, *Two-Dimensional Phase Unwrapping: Theory, Algorithms, and Software*, John Wiley and Sons, Inc, 1998.
19. R. Legarda-Sáenz, T. Bothe, and W. P. Jüptner, "Accurate procedure for the calibration of a structured light system," *Opt. Eng.* **43**(2), pp. 464-471, 2004.
20. Q. Hu, P. S. Huang, Q. Fu, and F. P. Chiang, "Calibration of a 3-d shape measurement system," *Opt. Eng.* **42**(2), pp. 487-493, 2003.
21. S. Zhang, *High-resolution, Real-time 3D Shape Measurement*. PhD thesis, State University of New York at Stony Brook, Stony Brook, NY, 11794, 2005.
22. J. Schwider, T. Dresel, and B. Manzke, "Some considerations of reduction of reference phase error in phase-stepping interferometry," *Appl. Opt.* **38**, pp. 655-658, 1999.
23. C. Joenathan, "Phase-measuring interferometry: New methods and error analysis," *Appl. Opt.* **33**, pp. 4147-4155, 1994.
24. P. Hariharan, "Phase-shifting interferometry: minimization of system errors," *Appl. Opt.* **39**, pp. 967-969, 2000.
25. K. Hibino, B. F. Oreb, D. I. Farrant, and K. G. Larkin, "Phase shifting for nonsinusoidal waveforms with phase-shift errors," *J. Opt. Soc. Am. A* **12**(4), pp. 761-768, 1995.
26. T. Maack and R. Kowarschik, "Camera influence on the phase measuring accuracy of a phase-shifting speckle interferometry," *Appl. Opt.* **35**(19), pp. 3514-3524, 1996.

27. P. L. Wizinowich, "Phase-shifting interferometry in the presence of vibration: a new algorithm and system," *Appl. Opt.* **29**(22), pp. 3266-3279, 1990.
28. B. Trolard, C. Gorecki, and G. M. Tribillon, "Speckle noise removal in interference fringes by optoelectronic preprocessing with epon liquid crystal television," in *Proc. of SPIE: in Laser Interferometry VIII: Techniques and Analysis*, **2860**, pp. 126-134, 1996.
29. S. Zhang and P. Huang, "Phase error compensation for a 3-d shape measurement system based on the phase-shifting method," in *Proc. SPIE, OpticsEast*, (Boston, MA), Oct. 2005.
30. F. J. Cuevas, M. Servin, and R. Rodriguez-Vera, "Depth object recovery using radial basis functions," *Opt. Commun* **163**(4), pp. 270-277, 1999.
31. F. J. Cuevas, M. Servin, O. N. Stavroudis, and R. Rodriguez-Vera, "Multi-layer neural networks applied to phase and depth recovery from fringe patterns," *Opt. Commun* **181**(4), pp. 239-259, 2000.
32. C. C. Slama, C. Theurer, and S. W. Henriksen, *Manual of Photogrammetry*, American Society of Photogrammetry, Falls Church, VA, 4th edition ed., 1980.
33. C. S. Fraser, "Photogrammetric camera component calibration: A review of analytical techniques," in *Calibration and Orientation of Camera in Computer Vision*, A. Gruen and T. S. Huang, eds., pp. 95-136, Springer-Verlag, (Berlin Heidelberg), 2001.
34. A. Gruen and H. A. Beyer, "System calibration through self-calibration," in *Calibration and Orientation of Camera in Computer Vision*, A. Gruen and T. S. Huang, eds., pp. 163-194, Springer-Verlag, (Berlin Heidelberg), 2001.
35. J. Heikkilä, "Geometric camera calibration using circular control," *IEEE Trans. Pattern Anal. Mach. Intell.* **PAMI-22**(10), pp. 1066-1077, 2000.
36. F. Pedersini, A. Sarti, and S. Tubaro, "Accurate and simple geometric calibration of multi-camera systems," *Signal Process* **77**(3), pp. 309-334, 1999.
37. D. B. Gennery, "Least-square camera calibration including lens distortion and automatic editing of calibration points," in *Calibration and Orientation of Camera in Computer Vision*, A. Gruen and T. S. Huang, eds., pp. 123-136, Springer-Verlag, (Berlin Heidelberg), 2001.
38. P. S. Huang, Q. Hu, F. Jin, and F. P. Chiang, "Color-encoded digital fringe projection technique for high-speed three-dimensional surface contouring," *Opt. Eng.* **38**, pp. 1065-1071, 1999.
39. P. Huang, S. Zhang, and F.-P. Chiang, "Trapezoidal phase-shifting method for 3-d shape measurement," in *Proc. SPIE, OpticsEast* **5606**, pp. 142-152, (Philadelphia, PA), Oct. 2004.
40. P. Huang and S. Zhang, "A fast three-step phase-shifting algorithm," in *Proc. SPIE, OpticsEast*, (Boston, MA), Oct. 2005.